PKC412 demonstrates JNK-dependent activity against human multiple myeloma cells

Janelle Sharkey,[1] Tiffany Khong,[1] and Andrew Spencer[1]

[1]Myeloma Research Group, The Alfred Hospital, Melbourne, Victoria, Australia

The effect and mode of action of the protein kinase C (PKC) inhibitor PKC412 on human multiple myeloma (MM) cell lines (HMCLs) and primary MM cells was explored. We found that PKC412 induced apoptosis of HMCLs and primary MM cells with variable efficacy; however, some activity was seen against all HMCLs and primary MM cells with at least 0.5 μM PKC412. PARP cleavage and decreased PKC activity was observed in all HMCLs tested. Furthermore, PKC412 inhibited *C-FOS* transcription and nuclear protein expression, induced reactive oxygen species (ROS) production, and induced both sustained *C-JUN* expression and phosphorylation. The latter was inhibited by cotreatment with the JNK inhibitor SP600125, which similarly abrogated PKC412-induced apoptosis, suggesting that PKC412-induced apoptosis is a JNK-dependent event. PKC412 treatment secondarily induced prosurvival stress responses as evidenced by activation of NFκB and increased expression of the heat shock proteins HSP70 and HSP90. Consistent with the former, sequential inhibition of NFκB activation with bortezomib or SN50 synergistically enhanced cell killing. Our results demonstrate that PKC412 induces JNK-dependent apoptosis of HMCLs and primary MM cells and that this effect is enhanced by NFκB inhibition. The further evaluation of PKC412 in the treatment of MM is justified. (Blood. 2007;109:1712-1719)

Introduction

Multiple myeloma (MM) is a B-cell malignancy, which occurs predominantly at an older age and is still incurable despite progress in treatment.[1] The investigation of novel anticancer drugs for the treatment of this disease is therefore warranted. Protein kinase C (PKC) is a phospholipid-dependent, serine/threonine kinase responsible for signal transduction in response to growth factors, hormones, and neurotransmitters.[2] PKC plays an important role in cell-growth regulation and tumor promotion[3] and has also been implicated in metastasis[4] and chemotherapy-associated multidrug resistance.[5] Total PKC activity has been reported to be elevated in carcinomas of breast[6] and lung.[7] In MM, PKC has been implicated in the shedding of CD138[8] and the IL-6 receptor,[9] both of which are thought to play important roles in tumor progression. Eleven isoforms of PKC have been identified, and these have been separated into 3 subgroups: (1) the conventional calcium-dependent and DAG (diacylglycerol)–dependent PKCs (cPKCs: α, β_I, β_{II}, γ), (2) the nonconventional calcium-independent but DAG-dependent PKCs (nPKCs: δ, ε, η, μ, θ), and (3) the atypical calcium-independent and DAG-unresponsive PKCs (aPKCs: ζ, λ).

The PKC inhibitor PKC412 (*N*-benzylstaurosporine) is a derivative of the naturally occurring alkaloid staurosporine and has been shown to inhibit the conventional isoforms of PKC (α, β_I, β_{II}, γ). PKC412 has been shown to have an antitumor effect on human non–small-cell lung cancer cells[10] and myeloma cells[11,12] and has also been shown to inhibit growth factor–dependent *C-FOS* mRNA expression.[13] PKC412 has also shown antitumor activity in a murine model of myeloproliferative disease[14] as well as in an FGFR3 TDII–induced murine model of B-cell lymphoma.[11]

The AP-1 transcription factor consists of homodimers of Jun proteins or heterodimers of Fos and Jun proteins[15,16] and plays a key role in the regulation of expression of genes involved in DNA repair, cell proliferation, cell-cycle arrest, death by apoptosis, and tissue and extracellular matrix remodeling proteases.[17] Formation of AP-1 dimers requires activation by phosphorylation of c-Jun[18]; thus, c-Jun and AP-1 activities are regulated by c-Jun N-terminal phosphorylation through Jun N-terminal kinases (JNKs).[16] JNK belongs to the mitogen-activated protein kinase family[19] and has a known role in both drug[20] and stress-induced apoptosis.[21] *C-FOS* is an immediate early response gene that can be induced following activation of specific growth factor receptors[13] and is known to have a role in cell proliferation, differentiation, and transformation.[22]

In the present study, we show that PKC412 induces apoptosis of HMCLs and primary MM cells and that this is, in part, mediated by c-jun activation by JNK. Furthermore, by sequentially blocking the PKC412-induced secondary prosurvival stress response, enhanced tumor-cell killing can be achieved.

Materials and methods

Cell culture

The human myeloma cell lines (HMCLs) U266, RPMI-8226, NCI-H929, and LP-1 were obtained from the American Type Culture Collection (Rockville, MD). KMS-11 was a kind gift from Dr Takemi Otsuki from the Kawasaki Medical School, Kawasaki, Japan, and OPM2 was purchased

Submitted May 17, 2006; accepted September 19, 2006. Prepublished online as *Blood* First Edition Paper, October 10, 2006; DOI 10.1182/blood-2006-05-014092.

An Inside *Blood* analysis of this article appears at the front of this issue.

The publication costs of this article were defrayed in part by page charge payment. Therefore, and solely to indicate this fact, this article is hereby marked "advertisement" in accordance with 18 USC section 1734.

from the German Collection of Microorganisms and Cell Cultures (Braunschweig, Germany). These HMCLs were cultured in our laboratory in RPMI 1640 (JRH Biosciences, Brooklyn, VIC, Australia) with 10% iron-fortified fetal bovine serum (IF FBS) (JRH Biosciences), 50 U/mL penicillin, 50 μg/mL streptomycin, and 2.9 mg/mL L-glutamine (Invitrogen, Mount Waverley, VIC, Australia) (Complete RPMI). Cells were incubated at 37°C in 5% carbon dioxide.

Mononuclear cells (MNCs) were isolated from the bone marrow (BM) samples of patients with MM after obtaining informed consent. Bone marrow was spun at 500*g* for 10 minutes to pellet cells, and plasma was collected. Pelleted cells were then resuspended in Iscove modification of Dulbecco medium (IMDM; JRH Biosciences) to 3 times the original sample volume, and DNase I was added to a final concentration of 1 μg/mL. The sample was then incubated for 30 minutes at room temperature, rolling. Ficoll-Hypaque Plus solution (Amersham Biosciences, Castle Hill, NSW, Australia) was layered under the BM sample so the volume of Ficoll solution was approximately one third the total volume in the tube. The BM sample was then spun at 800*g* for 25 minutes, and MNCs were collected from the Ficoll/IMDM interface. Red blood cells (RBCs) were lysed by incubation with RBC lysis buffer (8.29 g/L ammonium chloride, 0.037 g/L EDTA, 1 g/L potassium bicarbonate) for 5 minutes at 37°C. MNCs were washed twice with sterile PBS and were resuspended in complete RPMI and treated with PKC412 and/or bortezomib.

Reagents

PKC412 was kindly supplied by Novartis (Basel, Switzerland). It was dissolved in dimethyl sulfoxide (DMSO), stored at −20°C, and tested at 0.1 to 20 μM in the presence of culture medium with 10% IF FBS. Bortezomib was purchased from Janssen-Cilag (North Ryde, NSW, Australia), dissolved in 0.9% saline, and used at 8 nM. The JNK inhibitor SP600125 (Calbiochem, San Diego, CA) was dissolved in DMSO, stored at −20°C, and used at 25 μM. The NFκB inhibitor SN50 (Calbiochem, San Diego, CA) was dissolved in sterile water, stored at −20°C, and used at 25 μg/mL. 2′,7′-dichlorodihydrofluorescein diacetate (H_2DCFDA) (Molecular Probes, Eugene, OR) was formulated in methanol and used at a final concentration of 1 μg/mL; and L-*N*-acetylcyteine (LNAC) (Calbiochem) was dissolved in sterile water and used at a final concentration of 15 mM.

MTS assay

U266, LP-1, KMS-11, NCI-H929, OPM2, and RPMI-8226 cells (0.25×10^6/mL) were incubated with various concentrations of PKC412 (0.1-20 μM) for 24 and 72 hours in 96-well plates (Sarstedt, Ingle Farm, SA, Australia). After culture, cell number and viability were determined by 3-(4,5-dimethylthiazol-2-yl)-5-(3-carboxymethoxyphenyl)-2-(4-sulfophenyl)-2H-tetrazolium (MTS) assay (Pierce Biotechnology, Rockford, IL). Synergistic drug effects were quantified by calculation of the Synergism quotient (SQ).[23,24] The SQ is the net effect of the combination [drug A + drug B] divided by the sum of the net individual effect [A] + [B]. An SQ greater than 1 indicates a synergistic effect.

Assessment of apoptosis

To examine apoptotic-cell death, NCI-H929 and LP-1 cells were treated for 72 hours with (experiment 1) 4 μM PKC412, 25 μM SP600125, or both (SP600125 added 30 minutes prior to PKC412) or (experiment 2) 1 and 3 μM PKC412 and stained for flow cytometry with annexin V–FITC (BioSource, Camarillo, CA) and propidium iodide (Sigma, NSW, Australia). Cells were washed once in 2 mL annexin V binding (AB) buffer (0.01 M HEPES, 0.14 M NaCl, 2.5 mM $CaCl_2$, pH 7.4) and resuspended in 100 μL of this buffer, to which 1 μL annexin V–FITC was added. Cells were incubated in the dark for 15 minutes then washed once with 2 mL AB buffer. Cells were then resuspended in 300 μL AB buffer with 18.75 ng propidium iodide and analyzed by flow cytometry (Becton Dickinson FACScan; BD Biosciences, San Jose, CA). Data were analyzed using Expo 32 software (Beckman Coulter, Gladesville, NSW, Australia).

Assessment of primary myeloma-cell death

BM MNCs isolated from patients with MM were treated with PKC412 and/or bortezomib for 72 hours and were harvested for analysis by flow cytometry. Cells were washed in PBS, then resuspended in 100 μL PBS, and incubated for 10 minutes with Intragam P (1:50) (CSL Biosciences, Parkville, VIC, Australia). Anti–human CD138 FITC-conjugated antibody (BD Biosciences) and anti–human CD38 PE-conjugated antibody (BD Biosciences) were then added at 1:20 dilution, and cells were incubated in the dark for 15 minutes. Cells were then washed twice with 2 mL PBS and resuspended in 200 μL PBS with propidium iodide (PI) at 0.0625 μg/mL and analyzed by flow cytometry (Becton Dickinson FACScan, BD Biosciences) to identify $CD38^+/CD138^+/PI^+$ or $CD38^+/CD138^+/PI^-$ cells. Data were analyzed using Expo 32 software (Beckman Coulter).

Protein kinase C functional assay

PKC activity after 24 and 72 hours of treatment with 5 μM PKC412 was determined using the PepTag assay for nonradioactive detection of PKC (Promega, Madison, WI) according to the manufacturer's directions. Briefly, this assay uses a brightly colored, fluorescent peptide substrate that is highly specific for PKC. Phosphorylation by PKC of the specific peptide substrate alters the peptide's net charge from +1 to −1. This change in the net charge of the substrate allows the phosphorylated and nonphosphorylated versions of the substrate to be rapidly separated on a 1% agarose gel. The phosphorylated peptide migrates toward the positive electrode, whereas the nonphosphorylated peptide migrates toward the negative electrode. The gel is then photographed using UV illumination, and the amount of phosphorylated peptide (proportional to the amount of functional PKC) is determined by densitometry.

Reverse transcriptase–polymerase chain reaction (RT-PCR)

RNA was extracted from cells using the RNeasy RNA extraction kit (Qiagen, Doncaster, VIC, Australia) and cDNA synthesized using the Sensiscript RT kit (Qiagen) following the manufacturer's directions. *C-FOS* and *β-ACTIN* PCRs were performed using the following cycling conditions: 95°C 2 minutes (1 cycle); 95°C 1 minutes, 60°C 1 minute, 72°C 1 minute (30 cycles); 72°C 7 minutes (1 cycle). Primers were as follows: *C-FOS* downstream, TGA GAA GAG GCA GGG TGA AGG, and *C-FOS* upstream, CCG AAG GGA AAG GAA TAA GAT; *β-ACTIN* reverse, CAG CGG AAC CGC TCA TTG CCA ATG G, and *β-ACTIN* forward, TCA CCC ACA CTG TGC CCA TCT ACG TA. *C-JUN* PCR was performed using the following cycling conditions: 94°C 5 minutes (1 cycle); 94°C 30 seconds, 60°C 30 seconds, 72°C 1 minute (35 cycles); 72°C 10 minutes (1 cycle). Primers were as follows: *C-JUN* forward, AAA AGT GAA AAC CTT GAA AGC TCA G, and *C-JUN* reverse, CGT GGT TCA TGA CTT TCT GTT TAA G. PCR products were visualized using a 2% agarose gel. In all cases, equivalent quantities of cDNA template were used, and results were adjusted for variations in PCR efficiency by normalization to *β-ACTIN*.

Western blot analysis

After treatment cells were washed once with cold PBS and lysates were prepared using either NE PER nuclear and cytoplasmic extraction kit (Pierce Biotechnology) following the manufacturer's directions or RIPA buffer (10 mM Tris-HCl [pH 7.5], 150 mM NaCl, 1% vol/vol Triton X-100, 1% wt/vol sodium deoxycholate, 0.1% wt/vol SDS, 2 mM sodium vanadate, 10 mM sodium fluoride, 1 mM PMSF, complete EDTA protease inhibitor cocktail [Roche, NSW, Australia]). Proteins were resolved on 7% or 10% SDS polyacrylamide gels and transferred to a Hybond-C nitrocellulose membrane (Amersham, Arlington Heights, IL). Membranes were probed with antibodies where appropriate. Anti–c-Jun (Santa Cruz Biotechnology, Santa Cruz, CA), –p-c-Jun (Santa Cruz Biotechnology), –c-Fos (Santa Cruz Biotechnology), -PARP (Santa Cruz Biotechnology), -PKC α (Santa Cruz Biotechnology), -PKC β_I (Santa Cruz Biotechnology), -PKC β_{II} (Santa Cruz Biotechnology), -PKC γ (Santa Cruz Biotechnology), -p21 (Santa Cruz Biotechnology),

-p53 (Cell Signaling Technologies, Beverly, MA) and –α-tubulin (Sigma) antibodies were used to probe membranes. The blots were developed using the Supersignal west pico or dura chemiluminescent reagents (Pierce Biotechnology).

ROS production assay

Following treatment with PKC412 (5 μM) and with or without 2-hour pretreatment with 4 mM LNAC, HMCLs were incubated with H_2DCFDA at 1 μg/mL in the dark for 20 minutes at 37°C. Cells were then washed thoroughly with PBS and analyzed by flow cytometry (Becton Dickinson FACScan; BD Biosciences). Increased dye uptake reflected an increase in ROS levels. Data were analyzed using Expo 32 software (Beckman Coulter).

NFκB transcriptional assay

NCI-H929 and LP-1 cells were treated with 1 and 3 μM PKC412 for 24 and 72 hours. Nuclear extracts were prepared using the NE PER nuclear and cytoplasmic extraction kit (Pierce Biotechnology) following the manufacturer's directions. Nuclear extract per sample (10 μg) was analyzed for nuclear translocation of p50/p65 using the NFκB p50/p65 transcriptional assay (Chemicon, Boronia, VIC, Australia) following the manufacturer's directions.

Transfections and luciferase assay

NCI-H929 and RPMI 8226 cells were plated into 24-well plates at a cell density of 0.6×10^6 per 500 μL and were transfected with the pNFκB-Luc plasmid from the PathDetect In Vivo Signal Transduction Pathway *cis*-Reporting System (Stratagene, La Jolla, CA) and phRL-SV40 plasmid (Promega) using Lipofectamine 2000 transfection reagent (Invitrogen). The phRL-SV40 plasmid was included to control for cell number and viability by measurement of its production of *Renilla* luciferase. Eighteen hours following transfection, cells were cultured with PKC412 (5 μM) or tumor necrosis factor α (TNF-α; 50 ng/mL) for 24 hours, at which time luciferase activity in cell lysates was measured. Similarly, NCI-H929 cells were transfected with the pAP-1-Luc plasmid (Stratagene) and phRL-SV40 plasmid. Eighteen hours following transfection, cells were cultured with PKC412 (5 μM) or TNF-α (50 ng/mL) for 24 hours, at which time luciferase activity in cell lysates was measured. Luciferase activity was measured using the Dual Luciferase assay system (Promega) and was normalized for cell number and viability by *Renilla* luciferase activity. TNF-α treatment was used as a positive control for NFκB and AP-1 transcriptional activity (data not shown).

Measurement of heat shock protein 70 (HSP70) and HSP90 protein expression by flow cytometry

NCI-H929 and LP-1 cells were treated with 5 μM PKC412 or DMSO (1:1000) for 30 minutes, 4 hours, and 20 hours. After these times cells were harvested, washed in PBS, and fixed in 100 μL 2% paraformaldehyde/PBS for at least 1 hour at 4°C. Cells were then washed in 2 mL PBS and resuspended in 100 μL permeabilization buffer (0.5% saponin dissolved in 1% FCS/PBS) containing the primary antibody (rabbit anti-HSP70 [Cell Signaling Technology, Danvers, MA] or rabbit anti-HSP90 [Cell Signaling Technology]) at a dilution of 1:200, and incubated at room temperature for 30 minutes. Cells were then washed in 2 mL PBS and resuspended in 100 μL permeabilization buffer containing the secondary antibody (goat anti–rabbit IgG–FITC [Caltag Laboratories, Burlingame, CA]) at 1:200, and incubated at room temperature in the dark for 30 minutes. Cells were then washed with 2 mL PBS, resuspended in 300 μL PBS, and analyzed by flow cytometry (Becton Dickinson FACScan; BD Biosciences). Data were analyzed using Expo 32 software (Beckman Coulter).

The use of bone marrow mononuclear cells from human patients with multiple myeloma for this project was granted approval by the Alfred Hospital Ethics Committee.

Results

PKC412 induces apoptosis of HMCLs and primary MM cells

HMCLs were treated with PKC412 for 24 to 72 hours with a decrease in cell proliferation seen at doses of at least 0.5 μM (Figure 1A). Following 72 hours of 5 μM PKC412 the 4 HMCLs (OPM2, NCI-H929, KMS-11, and RPMI-8226) harboring activating mutations of either *RAS* or *FGFR3* (Ras/FGFR3-positive) were clearly more sensitive than the HMCLs (U266 and LP-1) without either activating mutation (Ras/FGFR3-negative) (Figure 1A) with the difference between each individual Ras/FGFR3-positive HMCL versus each negative HMCL being statistically significant (range, $P = .019$ to $P < .001$, Student t test) (see legend to Figure 1A). Similarly, the IC_{50}s of all 4 Ras/FGFR3-positive HMCLs (0.4-2.9 μM) were lower than their negative counterparts (4.1-4.6) (Table 1). Primary MM cells from 4 patients at the time of relapse were treated with PKC412 in coculture with patient-derived bone marrow stromal cells (BMSCs). All demonstrated sensitivity to 0.5 μM PKC412 after 72 hours in a fashion similar to the HMCLs (Figure 5C).

Apoptosis induction was confirmed in NCI-H929 and LP-1 when treated with 1 and 3 μM PKC412 for 72 hours as determined by annexin V staining (Figure 1B). Similarly, whole-cell lysates from NCI-H929 and LP-1 demonstrated PARP cleavage at both 24 and 72 hours after PKC412 (Figure 1C). The PepTag assay for nonradioactive detection of PKC demonstrated the expected decrease in PKC activity in all 3 HMCLs tested (NCI-H929, OPM2, and U266) (Figure 1D); however, Western blots demonstrated no apparent correlation between basal PKC expression levels or the pattern of PKC isoform expression and sensitivity to PKC412 (summarized in Table 1). Induction of both p21 and p53 was seen in PKC412-treated HMCLs (data not shown); however, this did not correlate with the level of apoptosis induced, suggesting that PKC412-induced apoptosis is not significantly p53/p21 dependent (data not shown). This is further supported by the efficacy of PKC412 against HMCLs (KMS-11 and U266) that do not express wild-type p53 (data not shown).

PKC412 induces discordant c-fos and c-jun expression and increased AP-1 activation

On the basis of the possible association of Ras/FGFR3 positivity with enhanced sensitivity to PKC412, the down-stream mediators of Ras/FGFR3 signaling, c-Fos and c-Jun, were evaluated. To determine the effect of PKC412 on *C-FOS* expression, HMCLs were stimulated with 100 nM PMA (phorbol 12-myristate 13-acetate) with or without prior PKC412 treatment. Pretreatment with PKC412 inhibited the PMA-induced increase in *C-FOS* mRNA as determined by RT-PCR (Figure 2A). Similarly, RT-PCR demonstrated down-regulation of basal *C-FOS* transcription (Figure 2B) that was also associated with reduced c-Fos nuclear protein expression as determined by Western blot (Figure 2C). Conversely, RT-PCR demonstrated that a single dose of PKC412 induced a sustained increase in *C-JUN* expression maintained for at least 20 hours (Figure 2D) that was associated with an increase in both the expression and phosphorylation of c-Jun protein (data not shown). Subsequently,

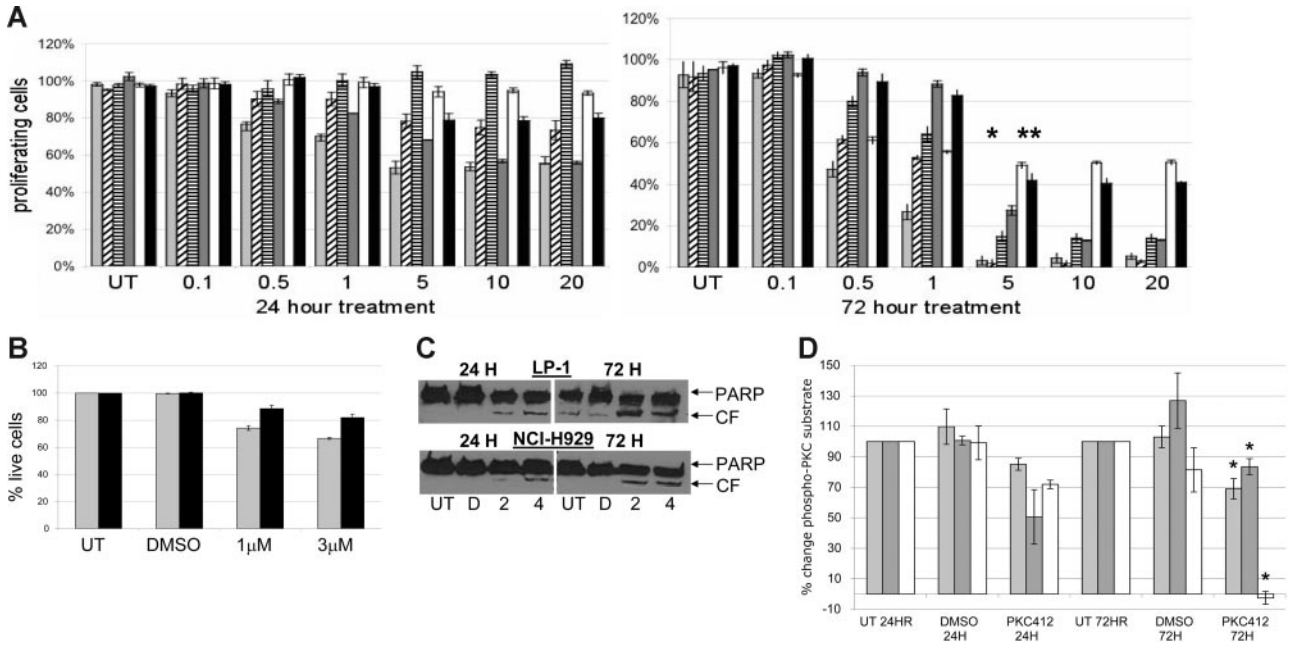

Figure 1. PKC412 induces apoptosis of HMCLs. (A) MTS assay data for HMCLs treated with PKC412 (0.1-20μM) for 24 and 72 hours. (▨ indicates NCI-H929; ▨, OPM2; ▤, RPMI-8226; [■], KMS-11; □, U266; and ■ LP-1). Graph represents data from 3 individual experiments *P values versus U266, **P values versus LP-1 [NCI-H929: *$P < .001$, **$P = .001$; OPM2: *$P < .001$, **$P < .001$; RPMI-8226: *$P < .001$, **$P = .002$; KMS-11: *$P < .001$, **$P = .019$], Student t test). (B) Live cells after 72 hours of treatment with 1 and 3 μM PKC412 was determined by annexin V–FITC/propidium iodide flow cytometry (▨ indicates NCI-H929; ■, LP-1). Graph represents data from 3 individual experiments. (C) Whole-cell lysates of cells treated with 2 μM (2) and 4 μM (4) PKC412 were analyzed for PARP cleavage by Western blot (CF indicates cleaved fragment; D, DMSO). Image is a representative of 2 experiments shown. (D) PKC activity in HMCLs measured after 24 and 72 hours of treatment with 5 μM PKC412 (▨ indicates NCI-H929; [■], OPM2; and □, U266; *$P = .009$, .036, and .001, respectively, versus untreated samples, Student t test, graph represents results from 3 experiments). Error bars for all graphs indicate standard error of the mean (SEM).

using a luciferase assay, AP-1 transcriptional activity was found to increase following PKC412 treatment in both HMCLs tested, NCI-H929 (Figure 2E) and RPMI 8226 (data not shown).

PKC412-induced apoptosis is preceded by the production of reactive oxygen species (ROS) and is partially JNK dependent

The effects of PKC412 on ROS generation were examined. As seen in Figure 3A, PKC412 induced an increase in ROS levels in both NCI-H929 and LP-1 as early as 15 minutes after treatment with PKC412, and the increase was sustained for at least 5 hours. This PKC412-induced increase in ROS production was inhibited by pretreatment with the free radical scavenger LNAC (Figure 3B). Published data have demonstrated that ROS-induced apoptosis is potentiated by JNK.[25,26] In view of this and the observed PKC412-induced up-regulation of *C-JUN*, we determined whether PKC-induced apoptosis was JNK dependent. Western blots of NCI-H929 and LP-1 whole-cell lysates following 4 μM PKC412 with or without 25 μM of the specific JNK inhibitor SP600125 demonstrated abrogation of both PKC412-induced expression and phosphorylation of c-Jun in the context of JNK inhibition (Figure 3C). Similarly, cotreatment of NCI-H929 and LP-1 with SP600125 significantly reduced PKC412-induced apoptosis ($P = .027$ and .043, respectively) (Figure 3D), confirming that PKC412-induced apoptosis is partially JNK dependent.

Table 1. Ras/FGFR3 status, baseline PKC/c-FOS levels, and PKC412 IC_{50}s for HMCLs

	U266	LP-1	RPMI-8226	OPM2	NCI-H929	KMS-11
PKC α	−	−	−	+	+	ND
PKC β_I	+	+	+	+	+	ND
PKC β_{II}	+	++	+	+/−	+	ND
PKC γ	−	−	−	−	+	ND
Activating *FGFR3* mutation	−	−	−	+	−	+
Activating *RAS* mutation	−	−	+	−	+	−
Total PKC expression	+/−	++	+	+++	+++	+++
Baseline *C-FOS* expression	++	+/−	+/−	+++	++	+/−
PKC412 IC_{50}, μM	4.6	4.1	1	0.75	0.4	2.9

Basal PKC and c-fos expression reported as not detected (−), weakly detected (+/−), detected (+), strongly detected (++), very strongly detected (+++) by Western blot/RT-PCR. PKC412 IC_{50} was determined using MTS assay (Promega). ND indicates not determined.

HMCLs exhibit prosurvival stress responses following treatment with PKC412

Stress-induced activation of the NFκB pathway and up-regulation of the HSP response may mitigate against drug- and radiation-induced apoptosis.[27,28] Inhibition of these induced prosurvival responses may thus theoretically enhance cell killing; therefore, the effect of PKC412 on NFκB and HSP was evaluated. As seen in Figure 4A and B, PKC412 induced significantly increased expression of both HSP70 (Figure 4A) and HSP90 (Figure 4B) compared with untreated controls ($P = .023$ and .020 for NCI-H929, and $P = .023$ and .027 for LP-1, respectively). To determine the effect of PKC412 on NFκB, nuclear translocation of NFκB was investigated. Treatment with 1 and 3 μM PKC412 for 72 hours induced a dose-dependent increase in nuclear translocation of NFκB (Figure 4C) with an apparent correlation between HMCL PKC412 sensitivity and the magnitude of PKC412-induced NFκB nuclear translocation: LP-1 (less PKC412 sensitive) 1.7-fold increase versus NCI-H929 (more PKC412 sensitive) 6.5-fold increase (Figure 4C). Increased NFκB transcriptional activation after PKC412 was confirmed using a luciferase assay for both NCI-H929 (Figure 4D) and RPMI 8226 (data not shown).

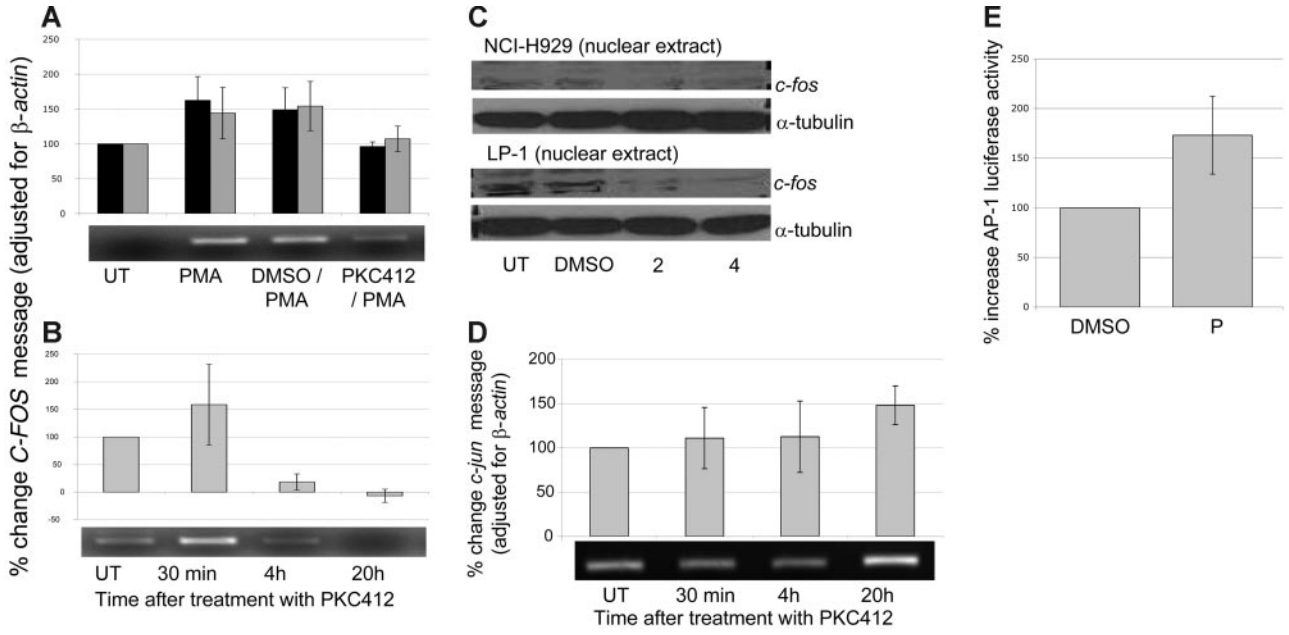

Figure 2. PKC412 induces modulation of c-fos and c-jun and increases AP-1 transcriptional activity. (A) RT-PCR of *C-FOS* following 90-minute pretreatment with PKC412 (10 μM) or DMSO (1:1000) followed by 30 minutes of PMA (100 nM) stimulation. (■ indicates LP-1; ▨, OPM2). Graph represents data from 2 individual experiments. Representative image shown. (B) RT-PCR of *C-FOS* following PKC412 (10 μM) for 30 minutes, 4 hours, and 20 hours (▨ indicates NCI-H929). Graph represents data from 2 individual experiments. Representative image shown. For both panels A and B, Scion Image (Scion, Frederick, MD) was used for densitometric analysis. (C) Reduction in nuclear expression of c-fos after 24 hours of treatment with 2 μM and 4 μM PKC412 was determined by Western blot. (D) RT-PCR of *C-JUN* after PKC412 (10 μM) treatment for 30 minutes, 4 hours, and 20 hours (▨ indicates NCI-H929). Graph represents data from 2 individual experiments. Representative image is shown. (E) PKC412 (P) (5 μM) treatment induces transcriptional activation of AP-1 as determined by luciferase assay (measured after 18 hours of treatment) (▨ indicates NCI-H929). Graph represents results from 2 experiments. Error bars for all graphs indicate SEM.

Pretreatment with PKC412 prior to NFκB inhibition induces synergistic killing of HMCLs and primary MM cells

The feasibility of exploiting the observed PKC412-induced stress-response to enhance MM-cell killing was evaluated. When NCI-H929 or OPM2 cells were treated with a combination of PKC412 and proteasome inhibitor bortezomib, there was greater cell death than with PKC412 alone (Figure 5A). The increment in cell killing with either PKC412 then bortezomib or bortezomib then PKC412 when compared with PKC412 alone was statistically significant for both HMCLs tested (NCI-H929, $P < .001$ and $P < .001$; OPM2, $P < .001$ and $P = .029$, respectively). However, the PKC412 then bortezomib sequence was clearly superior to bortezomib then PKC412 for both HMCLs (NCI-H929, $P = .024$; OPM2, $P = .013$). The calculated SQs for OPM2 for PKC412 then bortezomib or the

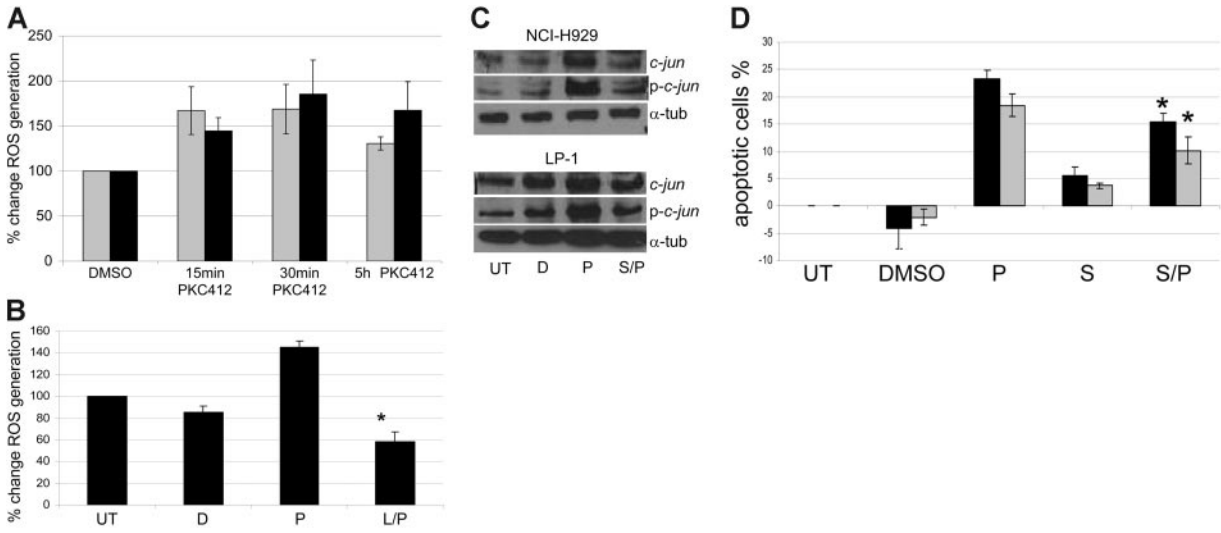

Figure 3. PKC412-induced apoptosis is preceded by the production of ROS and is JNK dependent. (A) Treatment with PKC412 (5 μM) induces ROS production in HMCLs measured by H_2DCFDA (1 μg/mL) fluorescence (▨ indicates NCI-H929; ■, LP-1). Graph represents data from 2 individual experiments. (B) PKC412-induced (5 μM for 30 minutes) ROS production was inhibited by 2 hours of pretreatment with LNAC (4 mM) as measured by H_2DCFDA (1 μg/mL) fluorescence (■ indicates LP-1; D, DMSO; P, PKC412; L, LNAC) (*$P = .0014$ versus PKC412 treatment, Student *t* test). Graph represents data from 3 individual experiments. (C) PKC412-induced (3 hours of treatment) modulation of c-jun and phosphorylation c-jun in HMCLs with and without pretreatment with the JNK-specific inhibitor SP600125 as shown by Western blot (P indicates PKC412; S, SP600125; D, DMSO). Representative image from 1 of 3 individual experiments is shown. (D) PKC412-induced apoptosis (4 μM PKC412) after 72 hours is partially abrogated by 30 minutes of pretreatment with SP600125 (25 μM) as determined by annexin V–FITC/PI flow cytometry of NCI-H929 (▨) and LP-1 (■). (*$P = .027$ and .043, respectively, versus PKC412 treatment alone, Student *t* test). Graph represents data from 3 individual experiments). Error bars for all graphs indicate SEM.

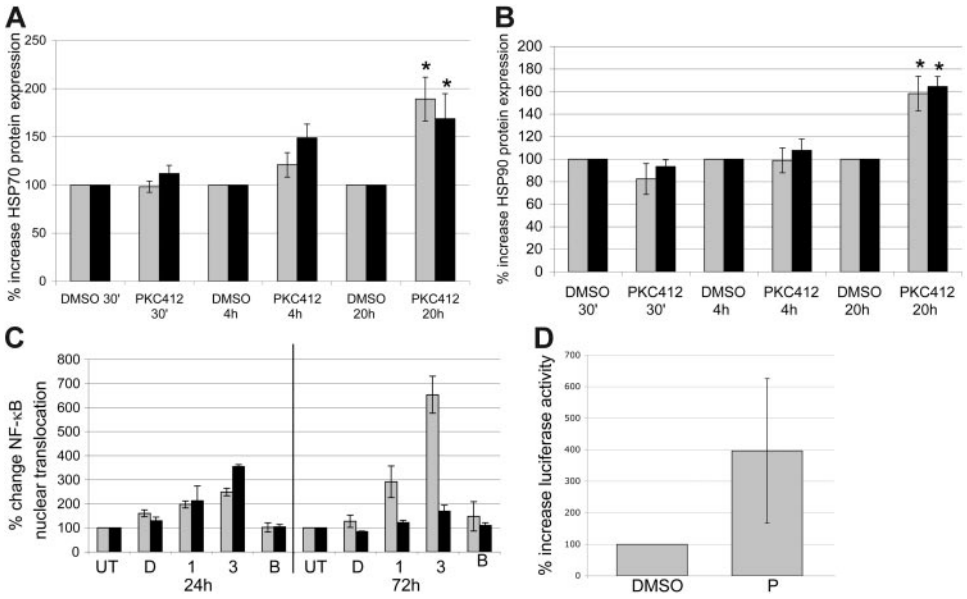

Figure 4. HMCL exhibit prosurvival stress responses following treatment with PKC412. (A) Treatment with PKC412 (5 μM) induces expression of HSP70 as measured by flow cytometry (▨ indicates NCI-H929; ■, LP-1; **P* = .023 and .026, respectively, versus DMSO treatment). Graph represents data from 3 individual experiments. (B) Treatment with PKC412 (5 μM) induces expression of HSP90 as measured by flow cytometry (▨ indicates NCI-H929; ■, LP-1; **P* = .020 and .027, respectively, versus DMSO treatment). Graph represents data from 3 individual experiments. (C) PKC412 treatment of the HMCL NCI-H929 induces NFκB activation as determined by p50/p65 nuclear translocation. Increased NFκB nuclear translocation is dose (1 μM versus 3 μM) and time (24 versus 72 hours) dependent (▨ indicates NCI-H929; ■, LP-1). Graph represents data from 3 individual experiments (bortezomib [B] was included as a negative control). (D) PKC412 (P) (5 μM) treatment induces transcriptional activation of NFκB as determined by luciferase assay (measured after 18 hours of treatment) (▨ indicates NCI-H929). Graph represents data from 3 individual experiments). Error bars for all graphs indicate SEM.

reverse order were 3.5 and 1.6, respectively. This is consistent with both combinations demonstrating synergy, but with PKC412 pretreatment prior to bortezomib demonstrating markedly greater synergy than the reverse order of administration. To determine whether the increase in cell death induced by cotreatment with bortezomib was in part secondary to NFκB inhibition,[29] we cotreated HMCLs (NCI-H929 and LP-1) with PKC412 and the NFκB inhibitor SN50. Greater killing was seen when cells were treated with a combination of PKC412 and SN50 than with either compound alone, although this was less than that seen with the bortezomib combination, likely because of the latter's broader range of action than SN50 (Figure 5B). Again the sequence using PKC412 first was superior in both cases. Similarly, treatment of all 4 primary MM samples demonstrated superior cell killing when using the same sequence of drug administration (Figure 5C). Importantly, the derived SQs for the PKC412 then bortezomib treatment of the primary MM cells were consistent with either synergistic or additive cell killing (MM016 SQ = 1.0; MM107 SQ = 2.0;, MM021 SQ = 1.6; and MM022 SQ = 1.0).

Discussion

PKC412 is an orally bioavailable staurosporine derivative capable of inhibiting a range of kinases[14,29] and has demonstrated safety in completed phase 1 trials.[30,31] We have demonstrated that PKC412 exerts an antiproliferative and apoptosis-inducing effect on both HMCLs and primary MM cells at doses of at least 0.5 μM. The activity of PKC412 in this context was associated with ROS generation, down-regulation of *C-FOS*, sustained up-regulation of phosphorylated c-Jun, and increased AP-1 transcriptional activity. Both sustained activation of c-Jun and apoptosis could be significantly abrogated by JNK inhibition. Finally, PKC412 treatment of HMCLs was associated with secondary prosurvival stress responses characterized by significant activation of NFκB signaling and elevations of HSP70 and HSP90. Targeting of the former with NFκB inhibitors in combination with PKC412 led to synergistic killing of both HMCLs and primary MM cells.

Examination of the HMCL responses demonstrated that the 4 Ras/FGFR3-positive HMCLs were more susceptible to PKC412 than the Ras/FGRF3-negative HMCLs (Figure 1). All exhibited lower IC_{50}s and in 3 of the 4 positive HMCLs the IC_{50}s were 4.5- to 11.5-fold lower than those of their Ras/FGFR3-negative counterparts (Table 1). Likewise, all the positive HMCLs demonstrated a statistically greater magnitude of cell killing at the 5-μm PKC412 dosing level than the negative HMCLs. Consistent with our observations, a study by Chen et al[11] showed that the IC_{50} for PKC412 was lower for t(4;14) MM cell lines that overexpress mutant FGFR3 than for those that do not.

Activating *RAS* and *FGFR3* mutations are mutually exclusive in MM,[32] suggesting a Ras-like role for FGFR3 in MM survival, proliferation, and tumor progression,[25] and recent insights into the role of c-Fos, c-Jun, and JNK in Ras signaling provide a possible basis for the enhanced sensitivity of the Ras/FGFR3-positive HMCLs to PKC412. Kang et al[33] reported that H-*RAS*–transformed human breast epithelial cells undergo apoptosis on caspain exposure in contrast to nontransformed counterparts.[28] Furthermore, capsaicin-induced apoptosis was mediated by modulation of Ras-downstream signaling molecules, including JNK activation. They were able to conclude that the presence of Ras enabled the selective killing of the transformed cells by caspain. Similarly, Xiao and Lang[34] reported that the JNK/c-Jun/AP-1 pathway mediates oncogenic Ras function in lung carcinoma cells, whereas Wang et al[35] have demonstrated a requirement for Ras for full activation of JNK by microtubule-interfering agents such as paclitaxel and vinblastine, again consistent with Ras-mediated sensitization to drug effects. Importantly, evidence suggests that sustained activation of JNK, as was seen in HMCLs secondary to PKC412

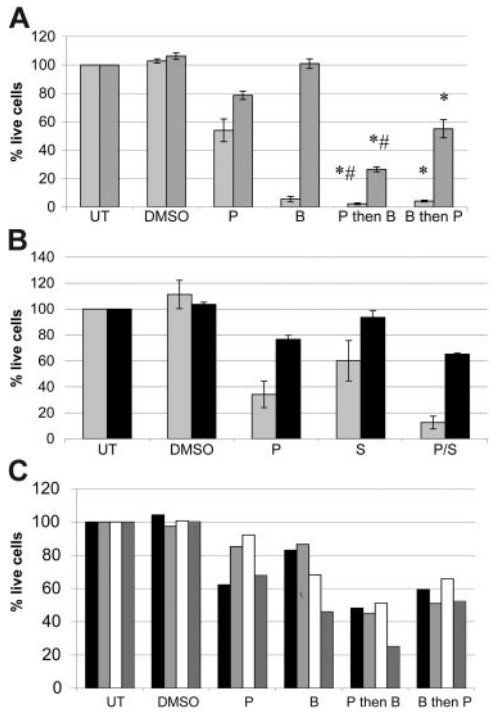

Figure 5. Synergistic killing induced by PKC412 and NFκB inhibition is schedule dependent. (A) Cotreatment with bortezomib (B) (8 nM) and PKC412 (P) (0.5 μM) enhances killing of HMCLs (▨ indicates NCI-H929; ■, LP-1) at 72 hours as measured by MTS assay. Graph represents data from 3 individual experiments. Combination treatments were 6 hours P pretreatment then B [P then B] or 6 hours B pretreatment then P [B then P]. NCI-H929, $^{*}P < .0015$ [P then B] and .001 [B then P], respectively, versus PKC412 alone; OPM2 $^{*}P < .001$ [P then B] and 0.029 [B then P], respectively, versus PKC412 alone. NCI-H929 $^{\#}P = .024$ [P then B] versus [B then P]; OPM2, $^{\#}P = .013$ [P then B] versus [B then P], Student *t* test. OPM2 SQ = 3.5 for [P then B] versus PKC412 alone and SQ = 1.6 for [B then P] versus PKC412 alone. (B) Cotreatment with SN50 (S) (25 μg/mL) and PKC412 (P) (1 μM) enhances killing of HMCLs (▨ indicates NCI-H929; ■, LP-1). Graph represents data from 3 individual experiments. (C) Seventy-two hours of treatment with PKC412 (0.5 μM) induces apoptosis in primary MM cells, and killing was enhanced by cotreatment with bortezomib (8 nM) (■ indicates patient MM016; ▨, patient MM017; □, patient MM021; and [■], patient MM022). SQs for [P then B] were 1.0, 2.0, 1.6, and 1.0, respectively. Error bars for all graphs indicate SEM.

treatment, can initiate the apoptotic process, whereas transient JNK activation may have a role in cell proliferation.[36] Finally, it has been reported that up-regulation of c-Fos by Ras is an important downstream mediator of the proliferative effects of Ras,[37] and recent data have demonstrated a critical role for c-Fos in the survival of transformed cells.[22]

These observations combined with our data are consistent with PKC412-induced apoptosis of HMCLs being, at least in part, secondary to modulation of c-Fos and c-Jun signaling downstream of Ras. The enhanced sensitivity of Ras/FGFR3-positive HMCLs, despite similar magnitudes of signaling changes in the Ras/FGFR3-negative HMCLs, would be explained by the greater reliance of the Ras/FGFR3-positive HMCLs on the integrity of Ras/FGFR3 downstream signaling in contrast to the negative HMCLs, where such pathways may not serve a critical function in terms of cell survival and proliferation (eg, IL-6–dependent HMCL U266). Thus, despite the pleiotropic nature of PKC412-induced cellular changes, the interference with downstream components of the Ras/FGFR3 pathway may provide the basis for our observations and provides a rationale for the investigation of PKC412-targeted therapy of Ras/FGFR3-positive MM.

ROS production has been shown to have a role in stress signaling by potentiating JNK activation[25,26,38]; however, coincident prosurvival NFκB activation may abrogate apoptosis induction as shown in work evaluating the potential of histone deacetylase inhibition as a therapeutic strategy in *BCR-ABL*–positive leukemias.[27] Despite the recognized role of PKC activation in the up-regulation of NFκB signaling,[39] the overall effect of HMCL exposure to PKC412 was marked enhancement of NFκB activation (1.7- to 6.5-fold increase), again reflecting the pleiotropic effect of PKC412 treatment. Further evidence of a significant stress response was the significant elevation of both HSP70 and HSP90 within 24 hours of PKC412 exposure. Therefore, strategies capable of effectively inhibiting this secondary prosurvival stress response should enhance PKC412-cell killing. This was clearly shown by combining PKC412 with bortezomib and recapitulated by combination studies with the specific NFκB inhibitor SN50. Importantly, the PKC412-bortezomib combination induced synergistic killing of not only HMCLs but also primary MM cells in BMSC cultures. These data are consistent with observations from Chunrong et al[27] who showed that the NFκB inhibitor Bay 11-7082 was able to reproduce bortezomib's ability to potentiate SAHA lethality in the K562 chronic myelocytic leukemia cell line.

We also showed that in both HMCLs and primary MM cells the magnitude of killing was greatest with PKC412 pretreatment prior to NFκB inhibition, rather than the reverse order, highlighting the importance of sequence of drug administration. Similarly, Mitsiades et al[40] have reported that when the HMCL MM.1S was pretreated with doxorubicin for 24 hours prior to the addition of bortezomib, greater cell killing was seen than with the reverse sequence. Likewise, Fahy et al[41] reported that the sequence of administration when using gemcitabine and bortezomib was crucial, with enhanced killing of pancreatic cancer cells occurring with gemcitabine followed by bortezomib. Although we have not attempted to fully optimize the scheduling and dosing of PKC412 and NFκB inhibition, we have provided a framework for such an evaluation to be performed. Furthermore, the demonstration of an HSP stress response subsequent to PKC412 treatment provides a rationale for the exploration of PKC412 and HSP inhibitor combination approaches. The latter, at least theoretically, is particularly attractive in view of the demonstrable preclinical activity of single-agent HSP inhibition against MM.[42]

In conclusion, we have demonstrated that PKC412 demonstrates activity against a range of genetically heterogenous HMCLs and primary MM cells and that this process is largely mediated by JNK. Furthermore, PKC412 provokes a marked prosurvival stress response. This provides the basis for rationally selected potential therapeutic combinations as demonstrated by the synergistic killing of MM cells by sequential exposure to PKC412 and NFκB inhibition. These data provide a rationale for the clinical evaluation of PKC412 both as a single agent and in combination with other available novel targeted therapeutics.

Acknowledgement

We would like to thank Mrs Karly Sourris for help with flow cytometry.

Authorship

Contribution: J.S. participated in designing and performing the research, analyzed the data, and wrote the paper; T.K. participated in performing the research; A.S. designed the research, analyzed

the data, and wrote the paper; and all authors checked the final version of the manuscript.

Conflict-of-interest disclosure: The authors declare no competing financial interests.

Correspondence: Andrew Spencer, Myeloma Research Group, Ground Floor, South Block, Alfred Hospital, Commercial Rd, Melbourne VIC 3004, Australia; e-mail: aspencer@netspace.net.au.

References

1. Kyle RA. Diagnosis of multiple myeloma. Semin Oncol. 2002;29:2-4.
2. Basu A. The potential of protein kinase C as a target for anticancer treatment. Pharmacol Ther. 1993;59:257-280.
3. Dean NM, McKay R, Condon TP, Bennett CP. Inhibition of protein kinase C-α expression in A549 cells by antisense oligonucleotides inhibits induction of intercellular adhesion molecule1 (ICAM-1) mRNA by phorbol esters. J Biol Chem. 1994;269: 16416-16424.
4. Herbert JM. Protein kinase C: a key factor in the regulation of tumour cell adhesion to the endothelium. Biochem Pharmacol. 1993;45:527-537.
5. Blobe GC, Sachs CW, Khan WA, et al. Selective regulation of expression of protein kinase C (PKC) isoenzyme in multidrug resistant MCF-7 cells: functional significance of enhanced expression of PKC-α. J Biol Chem. 1993;268:658-664.
6. O'Brian CA, Vogel VG, Singletary SE, Ward NE. Elevated protein kinase C expression in human breast tumor biopsies relative to normal breast tissue. Cancer Res. 1989;49:3215-3217.
7. Hirai M, Gamou S, Kobayashi M, Shimizu N. Lung cancer cells often express high levels of protein kinase C activity. Jpn J Cancer Res. 1989; 80:204-208.
8. Holen I, Drury NL, Hargreaves PG, Croucher PI. Evidence of a role for a non-matrix-type metalloproteinase activity in the shedding of syndecan-1 from human myeloma cells. Br J Haematol. 2001; 114:414-421.
9. Thabard W, Collette M, Bataille R, Amiot M. Protein kinase C δ and η isoenzymes control the shedding of the interleukin 6 receptor α in myeloma cells. Biochem J. 2001;358:193-200.
10. Ikegami Y, Yano S, Nakao K. Antitumour effect of CGP41251, a new selective protein kinase C inhibitor, on human non-small cell lung cancer cells. Jpn J Pharmacol. 1996;70:65-72.
11. Chen J, Lee BH, Williams IR, et al. FGFR3 as a therapeutic target of the small molecule inhibitor PKC412 in hematopoietic malignancies. Oncogene. 2005;24:8259-67.
12. Bahlis NJ, Miao Y, Koc ON, Lee K, Boise LH, Gerson SL. N-Benzoylstaurosporine (PKC412) inhibits AkT kinase inducing apoptosis in multiple myeloma cells. Leuk Lymphoma. 2005;46:899-908.
13. Andrejauskas-Buchdunger E, Regenass U. Differential inhibition of the epidermal growth factor-, platelet-derived growth factor-, and protein kinase C-mediated signal transduction pathways by the Staurosporine derivative CGP 41251. Cancer Res. 1992;52:5353-5358.
14. Chen J, DeAngelo DJ, Kutok JL, et al. PKC412 inhibits the zinc finger 198-fibroblast growth factor receptor 1 fusion tyrosine kinase and is active in treatment of stem cell myeloproliferative disorder. Proc Natl Acad Sci U S A. 2004;101:14479-14484.
15. Johnson R, Spiegelman B, Hanahan D, Wisdom R. Cellular transformation and malignancy induced by *ras* require *c-jun*. Mol Cell Biol. 1996; 16:4504-4511.
16. Behrens A, Sibilia M, Wagner EF. Amino-terminal phosphorylation of *c-jun* regulates stress-induced apoptosis and cellular proliferation. Nat Genet. 1999;21:326-329.
17. Tanos T, Marinissen MJ, Leskow FC, et al. Phosphorylation of *c-fos* by members of the p38 MAPK family: role in the AP-1 response to UV light. J Biol Chem. 2005;280:18842-18852.
18. Edwards J, Krishna NS, Mukherjee R, Bartlett MS. The role of *c-jun* and *c-fos* expression in androgen-independent prostate cancer. J Pathol. 2004;204:153-158.
19. Karin M. The regulation of AP-1 activity by mitogen-activated protein kinases. J Biol Chem. 1995; 270:16483-16486.
20. Yang Y, Ikezoe S, Saito T, Kobayashi M, Koeffler HP, Taguchi H. Proteasome inhibitor PS-341 induces growth arrest and apoptosis of non-small cell lung cancer cells via the JNK/*c-Jun*/AP-1 signaling. Cancer Sci. 2004;95:176-180.
21. Verheij M, Bose R, Lin XH, et al. Requirement for ceramide-initiated SAPK/JNK signalling in stress-induced apoptosis. Nature. 1996;380:75-79.
22. Lu C, Shen Q, DuPre E, Kim H, Hilsenbeck S, Brown PH. cFos is critical for MCF-7 breast cancer cell growth. Oncogene. 2005;24:6516-6524.
23. Beebe SJ, Holloway R, Rannels SR, Corbin JD. Two classes of cAMP analogs which are selective for the two different cAMP-binding sites of type II protein kinase demonstrate synergism when added together to intact adipocytes. J Biol Chem. 1984;259:3539-3547.
24. Tagliaferri P, Katsaros D, Clair T, Neckers L, Robins RK, Cho-Chung YS. Reverse transformation of Harvey murine sarcoma virus-transformed NIH/3T3 cells by site-selective cyclic AMP analogs. J Biol Chem. 1988;263:409-416.
25. Gao N, Rahmani M, Dent P, Grant S. 2-Methoxyestradiol-induced apoptosis in human leukemia cells proceeds through reactive oxygen species and Akt-dependent process. Oncogene. 2005;24:3797-3809.
26. Kim HJ, Chakravarti N, Oridate N, Choe C, Claret FX, Lotan R. N-(4-hydroxyphenyl)retinamide-induced apoptosis triggered by reactive oxygen species is mediated by activation of MAPLs in head and neck squamous carcinoma cells. Oncogene. 2006;25:2785-2794.
27. Chunrong Y, Rahmani M, Conrad D, et al. The proteasome inhibitor bortezomib interacts synergistically with histone deacetylase inhibitors to induce apoptosis in Bcr/Abl$^+$ cells sensitive and resistant to ST1571. Blood. 2003;102:3765-3774.
28. Dent P, Yacoub A, Contessa J, et al. Stress and radiation-induced activation of multiple intracellular pathways. Rad Res. 2003;158:283-300.
29. George P, Bali P, Cohen P, et al. Cotreatment with 17-allyamino-demethoxygeldanamycin and FLT-3 kinase inhibitor PKC412 is highly effective against human acute myelogenous leukaemia cells with mutant FLT-3. Cancer Res. 2004;64: 3645-3652.
30. Monnerat C, Henriksson R, Le Chevalier T, et al. Phase I study of PKC412 (N-benzoyl-staurosporine), an oral inhibitor of protein kinase C, combined with gemcitabine and cisplatin in patients with non-small-cell lung cancer. Ann Oncol. 2004; 15:316-323.
31. Eder JP, Garcia-Carbonero R, Clark JW, et al. A phase I trial of daily oral 4′-N-benzoyl-staurosporine in combination with protracted continuous infusion 5-fluorouracil in patients with advanced solid malignancies. Investigational New Drugs. 2004;22;139-150.
32. Chesi M, Brents LA, Ely SA, et al. Activated fibroblast growth factor receptor 3 is an oncogene that contributes to tumour progression in multiple myeloma. Blood. 2001;97:729-736.
33. Kang H-J, Soh Y, Kim M-S, et al. Roles of JNK-1 and p38 in selective induction of apoptosis by capsaicin in *ras*-transformed human breast epithelial cells. Int J Cancer. 2003;103:475-482.
34. Xiao L, Lang W. A dominant role for the *c-jun* NH_2-terminal kinase in oncogenic ras-induced morphologic transformation of human lung carcinoma cells. Cancer Res. 2000;60:400-408.
35. Wang T-H, Wang H-S, Ichijo H, et al. Microtubule-interfering agents activate *c-jun* N-terminal kinase/stress-activated protein kinase through both *ras* and apoptosis signal-regulating kinase pathways. J Biol Chem. 1998;273:4928-4936.
36. Chen YR, Wang X, Templeton D, Davis RJ, Tan TH. The role of *c-jun* N-terminal kinase (JNK) in apoptosis induced by ultraviolet C and γ radiation. J Biol Chem. 1996;271:31929-31936.
37. Gauthier-Rouviere C, Fernandez A, Lamb NJC. *ras*-induced *c-fos* expression and proliferation in living rat fibroblasts involves the C-kinase activation and the serum response element pathway. EMBO J. 1990;9:171-180.
38. Benhar M, Dalyot I, Engelberg D, Levitzki A. Enhanced ROS production in oncogenically transformed cells potentiates *c-jun* N-terminal kinase and p38 mitogen-activated protein kinase activation and sensitization to genotoxic stress. Mol Cell Biol. 2001;21:6913-6926.
39. Schutze S, Machleidt T, Kronke M. Mechanisms of tumor necrosis factor action. Semin Oncol. 1992;19:16-24.
40. Mitsiades NS, Mitsiades CS, Richardson PG, et al. The proteasome inhibitor PS-341 potentiates sensitivity of multiple myeloma cells to conventional chemotherapeutic agents: therapeutic applications. Blood. 2003;101:2377-2380.
41. Fahy B, Schlieman MG, Virudachalam S, Bold RJ. Schedule-dependent molecular effects of the proteasome inhibitor bortezomib and gemcitabine in pancreatic cancer. J Surg Res. 2003;113:88-95.
42. Mitsiades CS, Mitsiades NS, McMullan CJ, et al. Antimyeloma activity of heat shock protein-90 inhibition. Blood. 2006;107:1092-1100.